AUTOPHAGY PROTEIN LC3C BINDING TO PHOSPHOLIPID AND INTERACTION WITH LIPID MEMBRANES.

Uxue Ballesteros[1], Asier Etxaniz[1], Marina N. Iriondo[1], Yaiza R. Varela[1], Melisa Lázaro[2], Ana R. Viguera[1], L. Ruth Montes[1], Mikel Valle[2], Félix M. Goñi[1], Alicia Alonso[1]*

[1]Instituto Biofisika (CSIC, UPV/EHU) and Department of Biochemistry, University of the Basque Country, 48940 Leioa, Spain.

[2]CIC bioGUNE, Basque Research & Technology Alliance (BRTA), Bizkaia Technology Park, Building 800, 48160 Derio, Bizkaia, Spain.

*Corresponding author. Email: alicia.alonso@ehu.eus

ABSTRACT

Autophagy is a process in which parts of the eukaryotic cell are selectively degraded in the lysosome. The materials to be catabolized are first surrounded by a double-membrane structure, the autophagosome. Autophagosome generation is a complex event, in which many proteins are involved. Among the latter, yeast Atg8 or its mammalian orthologues are essential in autophagosome membrane elongation, shaping and closure. A subfamily of the human Atg8 orthologues is formed by the proteins LC3A, LC3B, and LC3C. Previous studies suggest that, at variance with the other two, LC3C does not participate in cardiolipin-mediated mitophagy. The present study was devoted to exploring the binding of LC3C to lipid vesicles, bilayers and monolayers, and the ensuing protein-dependent perturbing effects, in the absence of the mitochondrial lipid cardiolipin. All Atg8 orthologues are covalently bound to a phospholipid prior to their involvement in autophagosome elongation. In our case, a mutant in the C-terminal amino acid, LC3C G126C, together with the use of a maleimide-derivatized phosphatidyl ethanolamine, ensured LC3C lipidation, up to 100% under certain conditions. Ultracentrifugation, surface pressure measurements, spectroscopic and cryo-electron microscopic techniques revealed that lipidated LC3C induced vesicle aggregation (5-fold faster in sonicated than in large unilamellar vesicles) and inter-vesicular lipid mixing (up to 82%), including inner-monolayer lipid mixing (up to 32%), consistent with *in vitro* partial vesicle fusion. LC3C was also able to cause the release of 80-90% vesicular aqueous contents. The data support the idea that LC3C would be able to help in autophagosome elongation/fusion in autophagy phenomena.

INTRODUCTION

Autophagy (from the Greek auto-, "self" and phago, "to eat") is a general biological process conserved among eukaryotes that allows the regulated degradation of unnecessary or dysfunctional cellular materials. Autophagy was first detected in the 1950s [1]. It was originally observed as focal degradation of cytoplasmic areas performed by lysosomes. Later analysis revealed that autophagy starts with the sequestration of portions of the cytoplasm by a special double-membrane structure (termed the isolation membrane, or phagophore), which matures into the autophagosome (AP), also delimited by a double membrane. Subsequent fusion events expose the cargo to the lysosome (or the vacuole in fungi or plants) for enzymatic breakdown [2].

Two ubiquitin-like (UBL) conjugation systems participate in autophagosome membrane elongation, shaping and closure. These two systems, called for short Atg8 and Atg12, from one of their characteristic protein components, need to act in concert for a proper autophagosome elongation and sealing. The Atg8 protein is the central player and also the final effector of the Atg8 UBL system. A detailed description of this system can be seen in Yang and Klionsky [3], and in reviews by Mizushima et al. [4], and Lystad and Simonsen [5]. Atg8 orthologues are soluble proteins with molecular mass of approximately 17 kDa that are ubiquitously found in mammalian tissues and cultured cells. At least 7 Atg8 orthologues have been identified in mammals, divided into two subfamilies, LC3 and GABARAP. LC3A, LC3B and LC3C constitute the LC3 subfamily, whereas GABARAP, GABARAPL1/GEC1, GABARAPL2/GATE-16 and GABARAPL3 comprise the GABARAP one [6]. However, far from being simply redundant members of a protein family, specific members are suggested to act at different stages of autophagosome biogenesis [6]. During autophagosomal growth, a soluble form of LC3 (LC3-I) is conjugated to the phosphatidylethanolamine (PE) present in autophagosomal membranes to form an LC3-PE conjugate (LC3-II*)*. The lipidated product LC3-PE (or LC3-II) is considered as one of the main autophagy-specific markers in cells, and it is also one of the best known effectors in autophagosome elongation [6]. Atg8 proteins are instrumental in both AP formation and AP - lysosome fusion [7].

Several authors have approached autophagy, and particularly the fusion processes leading to AP growth, using model membrane systems consisting of vesicles of defined lipid compositions and purified proteins. Nakatogawa et al. [8] showed in a similar *in vitro* system that yeast Atg8 can trigger liposome tethering and hemifusion, whereas Weidberg et al. [9] found that mammalian orthologues of Atg8 have the same activities. Furthermore, Nair and co-workers [10] described how the *in vitro* fusion activity of Atg8-like proteins depended strongly on the presence of high amounts of PE (in the 50% mol range)[11]. In a previous report from this laboratory [12], two reconstituted systems were used, based on a minimal set of recombinant proteins together with synthetic vesicles of defined lipid compositions, to gain further insight into the ability of LC3/GABARAP to mediate membrane fusion. It was observed that both human LC3 and GABARAP subfamilies could be enzymatically lipidated *in vitro*.

As an alternative to the enzymatically driven reaction, a chemical conjugation approach involving 1,2-dioleoyl-*sn*-glycero-3-phosphatidylethanolamine-*p*-maleimidomethyl-cyclohexane carboxamide (PEmal) enables direct conjugation of proteins to PE lipids, thus bypassing the requirement for the conjugation machinery. Although the enzymatic conjugation

is more physiologically relevant, chemically conjugated versions of LC3/GABARAP subfamilies are easily prepared and are increasingly being used in autophagy studies [13, 14]. Landajuela et al. [12] reported that PEmal-conjugated LC3/GABARAP proteins faithfully recapitulate key features of their naturally conjugated homologs, supporting the reliable use of these artificial complexes.

In a further contribution [15], an analysis of LC3A, LC3B and LC3C interaction with cardiolipin (CL)-containing model membranes, and of their ability to translocate to mitochondria, has been performed. In the case of LC3C, even if this protein showed a stronger CL binding than LC3B or LC3A, the interaction was less specific, and colocalization of LC3C with mitochondria was not rotenone- or CCCP-dependent. Those results suggest that, at variance with LC3A or LC3B, LC3C does not participate in CL-mediated-mitophagy. Moreover, the interaction of LC3C with lipid bilayers not containing CL has not been characterized in detail, and it could provide light on the specific role of the LC3/GABARAP family in autophagy. LC3C has been shown to contain an amino-terminal extension, not present in other orthologues, that could mediate interaction with microtubules [16]. The present study was devoted to exploring the binding of LC3C to lipid vesicles, bilayers and monolayers, and the protein effects on the architecture and properties of the lipid assemblies. Ultracentrifugation, surface pressure measurements, spectroscopic and cryo-electron microscopic techniques were applied. The basic lipid mixture in our study contained egg phosphatidylcholine (PC), dioleoyl phosphatidylethanolamine (DOPE) and phosphatidylinositol (PI), following previous *in vitro* studies in this and other laboratories [8, 12]. PEmal was partially substituted for DOPE as required. A form of LC3C ending in the reactive C-terminal glycine, such that no ATG4-mediated preprocessing was necessary [12], was used in parallel with the mutant LC3C G126C that would allow interaction with PEmal.

MATERIALS AND METHODS

Materials

L-α-phosphatidylcholine from hen egg yolk (ePC, 840051), liver phosphatidylinositol (PI, 840042), 1,2-dioleoyl-*sn*-glycero-3-phosphatidylethanolamine-N-lissamine rhodamine B sulfonyl (Rho-PE, 810150), 1,2-dioleoyl-*sn*-glycero-3-phosphatidylethanolamine (DOPE, 850725), 1,2-dioleoyl-*sn*-glycero-3-phosphoethanolamine-N-[4-(p-maleimidomethyl)cyclohexane-carboxamide] (PEmal, 780201), and 1,2-dioleoyl-*sn*-glycero-3-phosphoethanolamine-N-(7-nitro-2-1,3-benzoxadiazol-4-yl) (NBD-PE, 810145) were purchased from Avanti Polar Lipids, Inc. (Alabaster, AL). *p*-Xylene-bis-pyridinium bromide (DPX, X-1525) and 8-aminonaphthalene-1,3,6-trisulfonic acid, disodium salt (ANTS, A350) were purchased from Thermo Fisher Scientific (Waltham, MA).

Protein assays

Protein concentration was estimated using a Nanodrop 2000 spectrophotometer from Thermo Fisher Scientific. Sample absorbance was measured at 800 nm and the concentration was calculated using the Lambert-Beer equation ($A = \varepsilon\ b\ c$; ε: 8940 $M^{-1}\ cm^{-1}$; b: 1cm).

Protein structure

Protein structure was monitored using circular dichroism in a J-810 spectropolarimeter (JASCO, Tokyo, Japan) equipped with a Jasco PTC-423 temperature controller. Proteins were diluted to 0,2 g/mL in System Buffer (50 mM Tris, 150 mM NaCl, pH 7.5) buffer. Protein concentration was

determined using a NanoDrop 2000 (Thermo Scientific, Waltham, MA). Samples were measured in a wavelength range of 200-250 nm in a 0.1-cm cuvette at 20 ºC, with a band pass of 1 nm. 40 spectra from each sample were accumulated to improve signal-to-noise ratio. Ellipticity was computed using the following equation:

$$\theta = (MRW * mDEG)/(10 * Cprot(\frac{g}{ml}) * L\ (cm)$$

Protein-denaturation temperature was determined from protein spectral data obtained in a low-salt buffer (5 mM Tris, 15 mM NaCl, pH 7.5) at 220 nm, in a 0.1-cm cuvette. Protein concentration was 0.2 mg/ml. Denaturation temperature was computed from the maxima of first derivative of the CD signal vs. temperature plot.

Recombinant LC3C expression and purification

The pGEX4T-1 plasmid for expression of human LC3C was kindly provided by Dr. Ivanna Novak (School of Medicine, University of Split, Croatia). The gene was a truncated form lacking the C-terminal Gly. The Gly-exposed form, such that no ATG4-mediated pre-processing was necessary, that was used in this work, was constructed using a QuikChange site-directed mutagenesis kit (Stratagene, San Diego, CA, 200514). To obtain LC3C G126C, the exposed Gly was mutated to a Cys through site-directed mutagenesis by Gene Script (Leiden, Netherlands). The mutation was confirmed by sequencing.

LC3C and LC3C G126C were purified from soluble fractions of bacterial extracts obtained in the absence of detergents, and they were >90% pure as evaluated by Coomassie Blue-stained SDS-PAGE. *E.coli* BL21(λDE3) cells were transformed with appropriate plasmids, grown to OD_{600}=0.8, and induced with 0.5 mM IPTG for 16 h at 20 ºC. Following centrifugation at 4,500 RCF for 15 min, the pellet was resuspended and sonicated in Breaking Buffer (phosphate buffered saline (PBS) with protease-inhibitor mixture and 1 mM DTT). After removal of cellular debris by centrifugation at 30,000 RCF for 30 min at 4 ºC, the sample supernatant fraction was incubated with 1 ml Glutathione Sepharose 4B (GE Healthcare, 17-0756-01) for 3 h at 4 ºC to bind the GST-tagged protein. Bound protein was cleaved with Thrombin Protease (GE Healthcare, 27-0846-01) overnight at room temperature in Thrombin Buffer (140 mM NaCl, 2.7 mM KCl, 10 mM Na_2HPO_4, 1.8 mM KH_2PO_4 (pH 7.3) with freshly added 1 mM DTT). After cleavage, LC3C was eluted in Assay Buffer (50 mM Tris- HCl pH 7.5, 150 mM NaCl, 1 mM EDTA with freshly added 1 mM DTT), then concentrated to 500 µl using Amicon Ultra-4 (4 mL, 3 kDa cut-off) (Millipore, Darmstadt, Germany, UFC800324), and loaded onto a Superdex75 10/300 GL size-exclusion column (GE Healthcare, Chicago, IL, GE17-5174-01) equilibrated in Assay Buffer supplemented with freshly added 1 mM DTT. The proteins were distributed in aliquots, flash-frozen, and stored in 20% glycerol at -80 ºC until further use. The secondary structures of LC3C and LC3C G126C were examined using circular dichroism, as detailed above. No differences were found between the two proteins (Fig. S1): in both cases α-helical contents were ≈11%, and the thermal denaturation temperature was ≈58.3 ºC.

Lipid monolayer measurements

Monolayers at the air-water interface in a Langmuir balance were studied at 25 °C as detailed elsewhere [17, 18]. In summary, lateral pressure experiments were carried out with a DeltaPi-4 system from Kibron (Helsinki, Finland) under constant stirring. The aqueous phase consisted of 1.25 mL 20 mM Tris-HCl, 150 mM NaCl, pH 7.5. The lipid, dissolved in chloroform:methanol (2:1),

was gently spread over the surface until the desired initial surface pressure was attained. Native and mutant LC3C proteins (2 µM) were injected with a micropipette through a hole connected to the subphase. The increment in surface pressure was recorded as a function of time until a stable signal was obtained. For these and other measurements, rates were obtained from Excel linear fits of the initial slopes of the individual curves.

Liposome preparation

The appropriate lipids (ePC:DOPE:PI, 35:55:10 mol ratio unless otherwise stated) were mixed in organic solution and the solvent was evaporated to dryness under a N_2 stream. Then the sample was kept under vacuum for 1 h to remove solvent traces. The lipids were swollen in System Buffer (150 mM NaCl, 50 mM Tris, pH 7.5) in order to obtain multilamellar vesicles (MLVs). Large unilamellar vesicles (LUV) were produced from MLV according to the extrusion method described by Mayer et al. [19] . They were subjected to 10 freeze/thaw cycles, and then extruded [LIPEX Liposome Extrusion System (Transferra Nanosciences, Burnaby, Canada)] using 0.1-µm pore size Nuclepore filters (Whatman, 110605). Small unilamellar vesicles (SUV) were obtained by sonicating MLV with a probe tip sonicator (MSE Soniprep 150, MSE, UK) for 20 min (10 sec on, 10 sec off) on ice. Vesicle size was checked by quasi-elastic light scattering using a Malvern Zeta-Sizer 4 spectrometer (Malvern Instruments, Malvern, UK). LUV had an average diameter of ≈100 nm and SUV average diameter was ≈50 nm. Phospholipid concentration was determined by phosphate analysis [20].

Vesicle flotation assay

Protein interaction with membranes was assessed using flotation in sucrose gradients [15]. Liposomes (3 mM), containing 0.05 mol% Rho-PE for detection, were incubated with 10 µM of the different purified proteins, for 1 h at 37 ºC in System Buffer pH 7.5 ,under continuous stirring (1100 rpm). The protein/lipid mix was adjusted to 1.4 M sucrose concentration in 300 µl and transferred to a centrifuge tube. This first (bottom) layer was overlaid with successive solutions containing 0.8 M (400 µl) and 0.5 M (300 µl) sucrose. The three-layer gradients were centrifuged in a TLA-120.2 rotor (Beckman Coulter, Brea, CA, US) at 355040 RCF (avg) for 50 min at 4 ºC. After centrifugation, four 250-µl fractions were collected, starting from the bottom. Proteins were detected in SDS-PAGE gels using Coomassie blue staining, and the presence of liposomes was monitored by measuring rhodamine (Rho-PE) fluorescence in a Synergy HT microplate reader (Bio-Tek, Winooski, VT). Densitometry of the protein bands was performed using ImageJ software, and the percent liposome-bound protein was estimated from the band intensities measured in the third + fourth fractions (floating vesicle fractions), relative to the total sum of intensities measured in all fractions.

Lipidation of LC3C G126C with PEmal

To assay LC3C-PE conjugation *in vitro* without the use of enzymes, purified LC3C G126C (5 µM) was incubated with 0 mol%, 20 mol% or 30 mol % PEmal-containing liposomes at a total final lipid concentration of 0.4 mM in System Buffer, pH 7.5. PEmal was a partial substitute for DOPE. The mixture was incubated at 37 ºC in System Buffer under continuous stirring (1100 rpm). 30 µL sample were taken at 0, 5, 10, and 60 min, then 6 µL Loading Buffer 6x were added to stop the reaction. The result was visualized by SDS-PAGE. The fraction of LC3C G126C-PE was estimated densitometrically using ImageJ software. The percent conjugated protein was calculated from the intensity of the fastest migrating band relative to the total intensity of the protein bands.

Aggregation assays

Liposome aggregation was monitored in a Varian Cary 300 (Agilent Technologies, Santa Clara, CA) spectrophotometer as an increase in turbidity (absorbance at 400 nm) of the sample. All assays were carried out in System Buffer pH 7.5, at 37°C with continuous stirring [12].

Cryo-EM sample preparation and image collection

LUVs with and without protein were incubated at 37ºC for 1 h with continuous stirring and then loaded on freshly glow-discharged 300-mesh R2/2 Quantifoil holey carbon grids (Quantifoil Micro Tools GmbH). Vitrification was performed on LEICA GP2 automatic plunge freezer (LEICA microsystems) maintained at 8 °C at a relative humidity close to saturation (90% rH). Grids were loaded with 4 µL sample solutions for 30 s, blotted with absorbent standard filter paper, and plunged into a liquid ethane bath. The vitrified grids were removed from the plunger and stored under liquid nitrogen.

Imaging of cryo-EM samples was made on a JEM-2200FS/CR (JEOL Europe, CIC bioGUNE, Spain) transmission electron microscope operated at 200 kV and images were recorded under low-dose conditions, with a total dose of the order of 30-40 electrons/Å² per exposure, at defocus values ranging from −1.5 to −4.0 µm. The in-column Omega energy filter of the microscope helps to record images with improved signal-to-noise ratio (SNR) by zero-loss filtering, using an energy selecting slit width of 20 eV centered at the zero-loss peak of the energy spectra. Digital images were recorded on a GATAN K2 summit direct detection camera 4K × 4K (5 µm pixels) (Gatan Inc., Pleasanton, CA) using DigitalMicrograph (Gatan Inc.) software, at a nominal magnification of 30,000×, resulting in final sampling of 1.3 Å/pixel.

Lipid mixing assays in large unilamellar vesicles

A fluorescence resonance energy transfer assay was used to monitor intervesicular membrane lipid mixing [27]. The appropriate LUVs containing 1.5 mol % NBD-PE and 1.5 mol % Rho-PE were mixed with a 9-fold excess of unlabeled LUVs. System Buffer, pH 7.5 was used. NBD-PE emission was monitored in a Aminco Bowman Series 2 spectrofluorometer (Thermo Fisher Scientific) in a thermostatically controlled 1-cm path length cuvette with constant stirring at 37°C. NBD emission was monitored at 530 nm with the excitation wavelength set at 465 nm (slits at 4 nm). A 515 nm cut-off filter was placed between the sample and the emission monochromator to avoid scattering interference. Inner monolayer lipid mixing was measured using asymmetrically labeled membrane vesicles produced by the quenching of the outer leaflet NBD-PE fluorescence upon addition of sodium dithionite [21]. Dithionite was removed by gel filtration in Sephadex G-25M, using System Buffer for elution. 100% intervesicular membrane lipid mixing and 100% inner-monolayer lipid mixing were established by adding 10µL of 10% (v/v) Triton X-100 to a final volume of 1 mL.

Vesicle contents leakage assay

Leakage of vesicle contents was monitored by the ANTS/DPX assay [22] at pH 7.5. ANTS emission was monitored at 520 nm with the excitation wavelength set at 355 nm (slits at 4 nm). To establish the 100% leakage signal, Triton X-100 was added to a concentration of 1%. Details for the vesicle contents leakage assay can be found in Goñi et al. [23].

Statistics

Unless otherwise stated all data are given as average values ± SE of three measurements obtained with different vesicle preparations. When required, statistical significance was measured with the Student's t-test.

RESULTS

Surface-active properties of LC3C

The surface-active properties of LC3C and LC3C G126C are shown in Fig. 1. Panels A and B reveal that both proteins were surface-active, since they increased the surface pressure at the air-buffer interface, indicating that at least a fraction of the added protein migrated to the interface. At least for the low protein concentrations, with which migration to the interface was relatively slow, the phenomenon was faster for LC3C G126C than for LC3C. This is clearly seen in the example at 0.1 μM protein concentration (Fig. 1A, B). Then the rate of protein adsorption to the interface increased with protein concentration (not shown) until the process appeared to become saturated with protein above 3-4 μM (Fig. 1C). The plot showed the maximum change in π caused by the peptide at about 15 mN/m.

Lipid-protein interaction was measured as follows [24]. Adding the appropriate amount of lipid onto the interface caused the surface pressure π to increase by the desired value (≈20 mN/m in this case) as the monolayer was established. The surface pressure π induced by the lipid monolayer must be equal to or higher than the maximum change in π caused by the protein, ≥15 mN/m in the present case. When the interface was occupied by a lipid monolayer compressed at ≈20 mN/m (Fig. 1D-G), protein addition to the subphase caused a further increase in π. This indicated that the protein was interacting with the lipid monolayer, i.e. part of the protein was becoming inserted in it, under conditions similar to those of the cell membranes. A semi-quantitative information of the process was obtained from the rate of π increase, reflecting the rate of protein insertion in the monolayer. The data summarized in Table 1 show that insertion was faster for LC3C G126C than for LC3C, and that, in the case of LC3C C126C, interaction occurred more readily with the monolayer containing PEmal. The above data prompted further studies of LC3C interaction with lipid bilayers.

LC3C conjugation to PE

In order to test *in vitro* LC3C lipidation, i.e. conjugation to PE, either native LC3C, or LC3C G126C, were incubated with 30 mol% PEmal-containing liposomes, and the vesicle-bound and non-bound proteins were separated by ultracentrifugation (flotation assay). The Gly-Cys substitution mimics the natural process in which LC3C is cleaved in its C-terminal end by Atg4, exposing a glycine. Next LC3C is associated with Atg7 and then transferred to Atg3 in an ATP-dependent trans-thioesterification process [25]. The results in Fig. 2 show that only the modified LC3C G126C form of the protein could bind the PEmal-containing liposomes to any sizable extent. Small unilamellar vesicles (SUV) and large unilamellar vesicles (LUV) appeared to be equally suitable for LC3C conjugation. Both PEmal and the G126C modification were required for LC3C conjugation to PE, in the absence of PEmal neither form of the protein could bind the liposomes (Supplementary Fig. S2).

In a different series of experiments, the lipidated and non-lipidated proteins were separated by electrophoresis, the conjugated form exhibiting a slightly higher mobility under our conditions. The quantitative data for chemical conjugation of LC3C G126C to PEmal are summarized in Fig.

3. Similar results were obtained with SUV and LUV, although in some cases conjugation was somewhat higher with SUV. Lowering the proportion of PEmal from 30 to 20 mol% in the vesicle membranes clearly decreased the proportion of lipidated LC3C G126C, and again no PE conjugation was observed in the absence of PEmal.

LC3C-induced vesicle aggregation

The capacity of LC3C, or of its LC3C G126C C-terminal variant, to promote vesicle aggregation was tested by measuring the change in turbidity (A_{400}) of a vesicle suspension. An increased turbidity (Rayleigh scattering) (Fig. 4) was interpreted as an increase in particle size due to vesicle aggregation [12, 23]. A much larger increase in turbidity was seen for SUV than for LUV when LC3C G126C was present. This might be due to the intrinsic tendency of the smaller vesicles to break down in a process of lysis and reassembly [26, 27], because of the higher lateral tension in the bilayer, as compared with LUV. The LC3C G126C variant, but not the native protein, was able to induce vesicle aggregation, an indication that, as occurs in the cellular environment, PE conjugation of LC3C was essential for vesicle aggregation. This was confirmed by the absence of aggregation (no change in turbidity) with vesicles containing PE, but not PEmal (Supplementary Fig. S3), making it impossible for LC3C G126C to bind the liposomes

Cryo-EM analysis

Vesicle aggregation induced by LC3C G126C could be demonstrated by cryo-EM observations, of which representative images are shown in Fig. 5, with additional galleries in Supplementary Fig. S4. Fig. 5 A,B were obtained from two grids, loaded with LUV composed of PC:DOPE:PEmal:PI (35:25:30:10) and incubated at 37ºC with LC3C G126C. Fig 5C represents similar LUV incubated with LC3C. Control vesicles, imaged in the absence of protein, are shown in Fig. 5D. Panels A,B, but not C or D, reflect events of vesicle aggregation, that were detected as an increase in vesicle suspension turbidity in Fig. 4. In addition to mere aggregation, instances are seen in Fig. 5A,B of vesicle-vesicle close contacts, with blurring of the individual bilayer structures, suggestive of inter-vesicular membrane fusion, even if vesicle size was not increased (see Fig. 5A,B). Electron-dense particles seen in Fig. 5, B, are difficult to interpret; those particles are commonly found whenever vesicles aggregat [28,29].

A caveat for the interpretation of the cryo-EM data is that the ice film in the holes of carbon film on the EM grid that holds the sample is extremely thin, of the same order of magnitude than the sample vesicles, and this can make visualizing the larger objects in the sample somewhat problematic. The setting might preselect vesicles and structures in these thin films that actually fit in the ice sheet, and this would lead to the experimenter not seeing an actual representation of the size distribution of the sample. While this is a significant point, it is also true that in other related systems examined in precisely the same way, structures of several hundred nm in length have been observed, even if perhaps underrepresented [12].

LC3C-induced inter-vesicle lipid mixing

Inter-vesicle lipid mixing can be easily monitored following standard fluorescence spectroscopy measurements [28]. Lipid mixing can occur either as a result of vesicle-vesicle fusion (or inter-vesicle fusion, or simply vesicle fusion), or else be secondary to what is called hemifusion [29] or close apposition [30] phenomena, in which the outer, but not the inner membrane lipids are exchanged between vesicles. Hemifusion can be distinguished from whole fusion measuring in similar samples both total lipid mixing and inner monolayer lipid mixing. The latter is a signature observation of vesicle fusion.

Total and inner-monolayer lipid mixing induced by LC3C and by LC3C G126C are shown in Fig. 6. With the variant protein that could be conjugated to PE both total and inner-monolayer lipid mixing were detected. Lipid mixing was more frequent in SUV than in LUV, probably because vesicle aggregation, a pre-requisite for intervesicular lipid mixing, was more clearly seen with SUV (Fig. 4). In both cases inner-monolayer lipid mixing was observed. With LC3C G126C and SUV the extent of inner-monolayer mixing was roughly one-half of the total lipid mixing (Fig. 6B), as expected from the total number of lipids involved in both cases. In the case of LUV, the extent of inner-monolayer mixing appeared to be larger than one-half (Fig. 6D), but in this case relative errors may be larger due to the small extent of total lipid mixing with LUV. The observed moderate amount of LUV lipid mixing with LC3C G126C, including inner-monolayer lipid mixing (Fig. 6D), is compatible with the degree of intervesicular membrane fusion seen by cryo-EM (Fig. 5 A,B). As with the previously discussed LC3C effects, the native protein was far less active than LC3C G126C (Fig. 6A,C). However, a small signal of lipid mixing was detected even with LC3C (Fig. 6A), perhaps a non-specific effect due to the surface-active character of this protein (see Fig. 1B-C). Moreover, as expected from the lack of aggregation seen in Supplementary Fig. S3, no lipid mixing was detected with vesicles in which DOPE, but not PEmal, was present (Supplementary Fig. S5).

LC3C-induced release of aqueous vesicle contents

The possible release of aqueous vesicle contents (vesicle leakage) as an effect of LC3C, or of LC3C G126C, was tested using the water-soluble molecules ANTS and DPX, and vesicles containing 30 mol % PEmal, as described under Methods. Representative experiments are shown in Fig. 7. Both LC3C and LC3C G126C induced a marked release of aqueous contents. LC3C G126C was clearly more effective in this respect, and the permeation rates were of the same order of magnitude in both LUV and SUV (Table 1). Again, the surface-active properties of LC3C (Fig. 1) can explain the membrane destabilization caused by the native protein. Moreover, neither the native nor the variant proteins were able to elicit any sizable release of aqueous contents from vesicles not containing PEmal (Supplementary Fig. S6).

The ANTS/DPX couple is often used to study the inter-vesicle mixture of aqueous contents, another marker of vesicle fusion together with the inner-monolayer lipid mixing. However, the large extent of aqueous contents release prevented reliable measurements of aqueous contents mixing in our system.

DISCUSSION

At least two experimental observations in this paper deserve a separate discussion. One is the membrane-perturbing effect of LC3C G126C, leading to lipid vesicle fusion, and the other is the requirement of LC3C modification into LC3C G126C to allow the said perturbing effect. This discussion will take into account quantitative data, summarized in Table 1, to provide additional detail to the representative experiments shown in Figs. 1-7.

Membrane perturbation induced by LC3C G126C

The LC3/GABARAP family of autophagy-related proteins, of which LC3C is a member, are known to bind the autophagosome and promote phagophore expansion and autophagosome-lysosome fusion [4, 5, 31]. Several authors have approached autophagy, and particularly the fusion processes leading to autophagosomal growth, using model membrane systems consisting of vesicles of defined lipid compositions and purified proteins. Nakatogawa et al. [8] showed in this kind of system that yeast Atg8 can trigger liposome tethering and hemifusion, whereas

Weidberg et al. [9] found that mammalian orthologues of Atg8 have the same activities. Furthermore, Nair and coworkers [10] described how the *in vitro* fusion activity of Atg8-like proteins depended strongly on the presence of high amounts of PE (in the 50% mol range) in the bilayers [11]. Studies from this laboratory [12, 32] have shown the ability of some human Atg8 orthologues (LC3B, GABARAP, and GATE-16) to mediate model membrane fusion. The present contribution is intended to extend the previous studies to the case of the Atg8 orthologue LC3C.

Demonstration of *in vitro* fusion requires the independent assay of vesicle aggregation, intervesicular mixing of total membrane lipids, mixing of inner monolayer lipids, and mixing of aqueous contents in the absence of vesicular content leakage or spill out [29, 33]. Mixing of aqueous contents is not an essential requirement because, in some cases, extensive leakage prevents this assay. Previous studies from this laboratory have shown examples of phospholipase C-promoted liposome fusion with [34] or without [35] leakage. In the present case, LC3C G126C has been shown to induce vesicle aggregation (Figs. 4, 5), total lipid mixing, and inner-monolayer lipid mixing (Fig. 6). The rates of inner lipid mixing induced by LC3C G126C are respectively 43% and 60% those of total lipid mixing in SUV and in LUV (from data in Table 1), i.e. rather close, considering technical errors, to the theoretical 50% that would ideally correspond to the proportion of lipids in the inner monolayer. This is enough to interpret the ensemble of results in terms of vesicle-vesicle fusion [34], even if the concomitant release of vesicle contents (Fig. 7) prevents the assay of aqueous contents mixing. The cryo-EM images are also suggestive of membrane fusion, even if, under the conditions, no vesicle growth is observed (Fig. 5 A,B). The situation is reminiscent of that of LC3/GABARAP family members in cardiolipin-dependent fusion [12], and it could reflect a physiologically relevant, moderate fusogenic activity of LC3C in the absence of cardiolipin.

In our recent study [15] differences in the lipid-protein interactions were shown between the orthologues LC3A, LC3B, and LC3C. LC3A and LC3B showed similar abilities to colocalize with mitochondria upon induction of cardiolipin externalization by rotenone in cultured mammalian cells, moreover results suggested a possible role of LC3A, but not of LC3B, in oxidized-cardiolipin recognition as a counterweight to excessive apoptosis. LC3C was not seen to interact with mitochondria in rotenone-dependent autophagy, or in the early stages of other autophagy processes. However the *in vitro* demonstration of LC3C-induced fusion of cardiolipin-free vesicles, described in this paper, suggests the involvement of this protein in other autophagy steps (elongation) different from recognizing cardiolipin as a signal in the early stages of mitophagy.

LC3C *vs*. LC3C G126C

All LC3/GABARAP proteins are considered to bind the growing autophagosome through a covalent bond, involving the protein C-terminus and (usually) PE [36-38]. In the cell, Atg8 conjugation to PE is achieved through a combination of enzyme activities. After activation by ATG4B, covalent attachment of LC3/GABARAP to PE is mediated by a ubiquitin-like chain of enzymatic steps involving the E1-like ATG7, E2-like ATG3, and E3-like ATG12-ATG5-ATG16. These reactions can be reconstituted *in vitro*, using recombinant purified proteins, liposomes and ATP [12, 14, 36]. Alternatively, LC3/GABARAP conjugation to PE can be achieved through a chemical method, involving a modified LC3/GABARAP protein, in which a C-terminal Cys replaces the native Gly (LC3C G126C), and a modified PE, that includes a reactive maleimide on its headgroup (PEmal). Importantly, Landajuela et al. [12] could detect the production of the lipidated products for three LC3/GABARAP proteins, LC3B, GABARAP, and GATE-16, both with the whole conjugation enzymatic system and using a chemically modified lipid. They further demonstrated

that both the enzymatically and chemically lipidated forms of the proteins exhibited similar effects on the lipid vesicles, in terms of membrane aggregation and fusion. These data justify the use of LC3C G126C as the activated form of LC3C in the present study. The capacity of LC3C G126C to react with PE has been demonstrated in this paper, using ultracentrifugation and SDS-PAGE (Figs. 2 and 3). Only LC3C G126C, and not LC3C, was able to bind vesicles containing PEmal (Figs. 2 and 3), and cause vesicle aggregation (Figs. 4, 5).

However, the native LC3C was not totally devoid of activity towards the lipid membranes: it could insert into lipid monolayers containing either PE or PEmal (Fig. 1D,E), it elicited a measurable amount of aqueous contents release from the vesicles (Fig. 7 and Table 1), and it even caused a small degree of lipid mixing with SUV (Fig. 6). These effects can be due to the surface-active nature of LC3C, comparable to that of LC3C G126C (Fig. 1A). The non-negligible release of aqueous contents in the presence of LC3C (Fig. 7), and even the small apparent mixing of lipids (Fig. 6), could in principle be attributed to a lytic, or solubilizing (detergent-like), effect of LC3C, that would somehow give rise to lipid-protein mixed micelles. However, even if this were the case, the weight of this process on the overall LC3C effects would be small, given the absence of a decrease in turbidity that would necessarily accompany solubilization (Fig. 4). The surface activity of this protein could explain the effects seen mainly in Fig. 7, although it is debatable whether or not these observations will have a correlation at the cellular level.

In a recent contribution, Maruyama et al. [40] described that enzymatic lipidation of *Saccharomyces cerevisiae* Atg8 on non-spherical giant vesicles induced a noticeable vesicle deformation into a sphere with an out-bud. This phenomenon was not observed with chemically lipidated Atg8. In the absence of further experiments with mammalian cells, the observation remains valid, and it might be an indication of Atg8-promoted phenomena other than membrane fusion, yet related to phagophore elongation.

In conclusion, the data in this paper support the notion that the mammalian Atg8-ortholog LC3C can play a role in the ubiquitin-like autophagy apparatus. The various known orthologues appear to have specialized functions, the peculiarity of LC3C would be to help in autophagosome elongation/fusion in autophagy steps (elongation) different from recognizing cardiolipin as a signal.

Credit authorship contribution statement. UB performed most of the experiments, with the help of A.E., M. N. I., and Y.V. A.R.V. carried out and interpreted the CD studies. L.R.M. helped in analyzing the results and planning further experiments. M.L. and M.V. carried out and analyzed the cryo-EM observations. F.M.G. and A.A. had the original idea, provided funding, and wrote a first draft. All authors discussed and edited the manuscript.

Declaration of competing interest. The authors declare no competing interests.

Acknowledgments. The authors are grateful to Dr. I. Novak (Split, Croatia) for the gift of pGEX4T-1 plasmid for expression of human LC3C, to Dr. E.J. Gonzalez-Ramirez for his help with SUV preparation, and to Ms. A. Marcos for excellent technical assistance. This work was supported in part by the Spanish Ministerio de Ciencia e Innovación (MCI), Agencia Estatal de Investigación (AEI) and Fondo Europeo de Desarrollo Regional (FEDER) (grant No. PGC2018-099857-B-I00), by the Basque Government (grants No. IT1625-22 and IT1270-19), by Fundación Ramón Areces (CIVP20A6619), by Fundación Biofísica Bizkaia, and by the Basque Excellence Research Centre (BERC) program of the Basque Government. M.N.I. and Y.V. were recipients of pre-doctoral FPU fellowships from the Spanish Ministry of Science, Innovation and Universities (FPU16/05873, FPU18/00799). U.B. thanks the University of the Basque Country for a pre-

doctoral contract. A.E. was a post-doctoral scientist supported by the Basque Government and by Ministerio de Ciencia e Innovación.

REFERENCES

[1] E.L. Eskelinen, F. Reggiori, M. Baba, A.L. Kovács, P.O. Seglen, Seeing is believing: The impact of electron microscopy on autophagy research, Autophagy. 7 (2011) 935–956. https://doi.org/10.4161/auto.7.9.15760.

[2] D.J. Klionsky, A. Kamal Abdel-Aziz, S. Abdelfatah, M. Abdellatif, A. Abdoli, S. Abel, H. Abeliovich, M.H. Abildgaard, Y. Princely Abudu, A. Acevedo-Arozena, I.E. Adamopoulos, K. Adeli, T.E. Adolph, A. Adornetto, E. Aflaki, G. Agam, A. Agarwal, B.B. Aggarwal, M. Agnello, P. Agostinis, J.N. Agrewala, A. Agrotis, P. v Aguilar, S. Tariq Ahmad, Z.M. Ahmed, U. Ahumada-Castro, S. Aits, S. Aizawa, Y. Akkoc, T. Akoumianaki, H. Aysin Akpinar, A.M. Al-Abd, L. Al-Akra, A. Al-Gharaibeh, M.A. Alaoui-Jamali, S. Alberti, E. Alcocer-Gómez, C. Alessandri, M. Ali, M. Abdul Alim Al-Bari, S. Aliwaini, J. Alizadeh, E. Almacellas, A. Almasan, A. Alonso, G.D. Alonso, N. Altan-Bonnet, D.C. Altieri, É.M. C Álvarez, S. Alves, C. Alves da Costa, M.M. Alzaharna, M. Amadio, C. Amantini, C. Amaral, S. Ambrosio, A.O. Amer, V. Ammanathan, Z. An, S.U. Andersen, S.A. Andrabi, M. Andrade-Silva, A.M. Andres, S. Angelini, D. Ann, U.C. Anozie, M.Y. Ansari, P. Antas, A. Antebi, Z. Antón, T. Anwar, L. Apetoh, N. Apostolova, T. Araki, Y. Araki, K. Arasaki, W.L. Araújo, J. Araya, C. Arden, M.-A. Arévalo, S. Arguelles, E. Arias, J. Arikkath, H. Arimoto, A.R. Ariosa, D. Armstrong-James, L. Arnauné-Pelloquin, A. Aroca, D.S. Arroyo, I. Arsov, R. Artero, D. Maria Lucia Asaro, M. Aschner, M. Ashrafizadeh, O. Ashur-Fabian, A.G. Atanasov, A.K. Au, P. Auberger, H.W. Auner, L. Aurelian, R. Autelli, L. Avagliano, Y. Ávalos, S. Aveic, C. Alexandra Aveleira, T. Avin-Wittenberg, Y. Aydin, S. Ayton, S. Ayyadevara, M. Azzopardi, M. Baba, J.M. Backer, S.K. Backues, D.-H. Bae, O.-N. Bae, S. Han Bae, E.H. Baehrecke, A. Baek, S.-H. Baek, S. Hee Baek, G. Bagetta, A. Bagniewska-Zadworna, H. Bai, J. Bai, X. Bai, Y. Bai, N. Bairagi, S. Baksi, T. Balbi, C.T. Baldari, W. Balduini, A. Ballabio, M. Ballester, S. Balazadeh, R. Balzan, R. Bandopadhyay, S. Banerjee, S. Banerjee, Á. Bánréti, Y. Bao, M.S. Baptista, A. Baracca, C. Barbati, A. Bargiela, D. Barilà, P.G. Barlow, S.J. Barmada, E. Barreiro, G.E. Barreto, J. Bartek, B. Bartel, A. Bartolome, G.R. Barve, S.H. Basagoudanavar, D.C. Bassham, R.C. Bast Jr, A. Basu, H. Batoko, I. Batten, E.E. Baulieu, B.L. Baumgarner, J. Bayry, R. Beale, Guidelines for the use and interpretation of assays for monitoring autophagy (4th edition) 1, n.d. https://www.tandfonline.com/loi/kaup20.

[3] Y. Yang, D.J. Klionsky, A novel reticulophagy receptor, Epr1: a bridge between the phagophore protein Atg8 and ER transmembrane VAP proteins, Autophagy. 17 (2021) 597–598. https://doi.org/10.1080/15548627.2020.1837457.

[4] N. Mizushima, T. Yoshimori, Y. Ohsumi, The role of atg proteins in autophagosome formation, Annual Review of Cell and Developmental Biology. 27 (2011) 107–132. https://doi.org/10.1146/annurev-cellbio-092910-154005.

[5] A.H. Lystad, A. Simonsen, Mechanisms and Pathophysiological Roles of the ATG8 Conjugation Machinery, Cells. 8 (2019). https://doi.org/10.3390/cells8090973.

[6] H. Weidberg, E. Shvets, T. Shpilka, F. Shimron, V. Shinder, Z. Elazar, LC3 and GATE-16/GABARAP subfamilies are both essential yet act differently in autophagosome biogenesis, EMBO Journal. 29 (2010) 1792–1802. https://doi.org/10.1038/emboj.2010.74.

[7] T.N. Nguyen, B.S. Padman, J. Usher, V. Oorschot, G. Ramm, M. Lazarou, Atg8 family LC3/GAB ARAP proteins are crucial for autophagosome-lysosome fusion but not autophagosome formation during PINK1/Parkin mitophagy and starvation, Journal of Cell Biology. 215 (2016) 857–874. https://doi.org/10.1083/jcb.201607039.

[8] H. Nakatogawa, Y. Ichimura, Y. Ohsumi, Atg8, a Ubiquitin-like Protein Required for Autophagosome Formation, Mediates Membrane Tethering and Hemifusion, Cell. 130 (2007) 165–178. https://doi.org/10.1016/j.cell.2007.05.021.

[9] H. Weidberg, T. Shpilka, E. Shvets, A. Abada, F. Shimron, Z. Elazar, LC3 and GATE-16 N Termini Mediate Membrane Fusion Processes Required for Autophagosome Biogenesis, Developmental Cell. 20 (2011) 444–454. https://doi.org/10.1016/j.devcel.2011.02.006.

[10] U. Nair, A. Jotwani, J. Geng, N. Gammoh, D. Richerson, W.L. Yen, J. Griffith, S. Nag, K. Wang, T. Moss, M. Baba, J.A. McNew, X. Jiang, F. Reggiori, T.J. Melia, D.J. Klionsky, SNARE proteins are required for macroautophagy, Cell. 146 (2011) 290–302. https://doi.org/10.1016/j.cell.2011.06.022.

[11] H. Laczkó-Dobos, A.K. Maddali, A. Jipa, A. Bhattacharjee, A.G. Végh, G. Juhász, Lipid profiles of autophagic structures isolated from wild type and Atg2 mutant Drosophila, Biochimica et Biophysica Acta (BBA) - Molecular and Cell Biology of Lipids. 1866 (2021) 158868. https://doi.org/10.1016/j.bbalip.2020.158868.

[12] A. Landajuela, J.H. Hervás, Z. Antón, L.R. Montes, D. Gil, M. Valle, J.F. Rodriguez, F.M. Goñi, A. Alonso, Lipid Geometry and Bilayer Curvature Modulate LC3/GABARAP-Mediated Model Autophagosomal Elongation, Biophysical Journal. 110 (2016) 411–422. https://doi.org/10.1016/j.bpj.2015.11.3524.

[13] P. Ma, J. Mohrlüder, M. Schwarten, M. Stoldt, S.K. Singh, R. Hartmann, V. Pacheco, D. Willbold, Preparation of a functional GABARAP-lipid conjugate in nanodiscs and its investigation by solution NMR spectroscopy, ChemBioChem. 11 (2010) 1967–1970. https://doi.org/10.1002/cbic.201000354.

[14] H. Nakatogawa, Y. Ohsumi, SDS-PAGE Techniques to Study Ubiquitin-Like Conjugation Systems in Yeast Autophagy, in: 2012. https://doi.org/10.1007/978-1-61779-474-2_37.

[15] M.N. Iriondo, A. Etxaniz, Y.R. Varela, J.H. Hervás, L.R. Montes, F.M. Goñi, A. Alonso, LC3 subfamily in cardiolipin-mediated mitophagy: A comparison of the LC3A, LC3B and LC3C homologs, BioRxiv. (2020). https://doi.org/10.1101/2020.07.14.202812.

[16] C. Krichel, C. Möckel, O. Schillinger, P.F. Huesgen, H. Sticht, B. Strodel, O.H. Weiergräber, D. Willbold, P. Neudecker, Solution structure of the autophagy-related protein LC3C reveals a polyproline II motif on a mobile tether with phosphorylation site, Scientific Reports. 9 (2019) 14167. https://doi.org/10.1038/s41598-019-48155-8.

[17] L. Sánchez-Magraner, A.R. Viguera, M. García-Pacios, M.P. Garcillán, J.L.R. Arrondo, F. de La Cruz, F.M. Goñi, H. Ostolaza, The calcium-binding C-terminal domain of Escherichia coli α-hemolysin is a major determinant in the surface-active properties of

the protein, Journal of Biological Chemistry. 282 (2007) 11827–11835. https://doi.org/10.1074/jbc.M700547200.

[18] H. Ahyayauch, M. Raab, J. v. Busto, N. Andraka, J.L.R. Arrondo, M. Masserini, I. Tvaroska, F.M. Goñi, Binding of β-amyloid (1-42) peptide to negatively charged phospholipid membranes in the liquid-ordered state: Modeling and experimental studies, Biophysical Journal. 103 (2012) 453–463. https://doi.org/10.1016/j.bpj.2012.06.043.

[19] L.D. Mayer, M.J. Hope, P.R. Cullis, Vesicles of variable sizes produced by a rapid extrusion procedure, Biochimica et Biophysica Acta (BBA) - Biomembranes. 858 (1986). https://doi.org/10.1016/0005-2736(86)90302-0.

[20] Fiske C.H., Subbarow Y., The colorimetric determination of phosphorus, J. Biol. Chem. . 66 (1925) 375–400.

[21] Y. Xu, F. Zhang, Z. Su, J.A. McNew, Y.-K. Shin, Hemifusion in SNARE-mediated membrane fusion, Nature Structural & Molecular Biology. 12 (2005). https://doi.org/10.1038/nsmb921.

[22] H. Ellens, J. Bentz, F.C. Szoka, Proton- and calcium-induced fusion and destabilization of liposomes, Biochemistry. 24 (1985). https://doi.org/10.1021/bi00334a005.

[23] F.M. Goñi, A. v Villar, J.L. Nieva, A. Alonso, Interaction of Phospholipases C and Sphingomyelinase with Liposomes, in: 2003. https://doi.org/10.1016/S0076-6879(03)72001-1.

[24] P. Calvez, S. Bussières, Éric Demers, C. Salesse, Parameters modulating the maximum insertion pressure of proteins and peptides in lipid monolayers, Biochimie. 91 (2009) 718–733. https://doi.org/10.1016/j.biochi.2009.03.018.

[25] N.N. Noda, K. Satoo, Y. Fujioka, H. Kumeta, K. Ogura, H. Nakatogawa, Y. Ohsumi, F. Inagaki, Structural basis of Atg8 activation by a homodimeric E1, Atg7, Molecular Cell. 44 (2011) 462–475. https://doi.org/10.1016/j.molcel.2011.08.035.

[26] Alonso A., Villena A., Goñi F.M., LYSIS AND REASSEMBLY OF SONICATED LECITHIN VESICLES IN THE PRESENCE OF TRITON X-100, FEBS Lett. 123 (1981) 200–204.

[27] A. Alonso, R. Sáez, A. Villena, F.M. Goñi, Increase in size of sonicated phospholipid vesicles in the presence of detergents, The Journal of Membrane Biology. 67 (1982). https://doi.org/10.1007/BF01868647.

[28] M.G. Lete, J. Sot, D. Gil, M. Valle, M. Medina, F.M. Goñi, A. Alonso, Histones Cause Aggregation and Fusion of Lipid Vesicles Containing Phosphatidylinositol-4-Phosphate, Biophysical Journal. 108 (2015) 863–871. https://doi.org/10.1016/j.bpj.2014.12.018.

[29] A. Rendón-Ramírez, M. Shukla, M. Oda, S. Chakraborty, R. Minda, A.M. Dandekar, B. Ásgeirsson, F.M. Goñi, B.J. Rao, A Computational Module Assembled from Different Protease Family Motifs Identifies PI PLC from Bacillus cereus as a Putative Prolyl Peptidase with a Serine Protease Scaffold, PLoS ONE. 8 (2013) e70923. https://doi.org/10.1371/journal.pone.0070923.

[30] D.K. Struck, D. Hoekstra, R.E. Pagano, Use of resonance energy transfer to monitor membrane fusion, Biochemistry. 20 (1981). https://doi.org/10.1021/bi00517a023.

[31] L. Chernomordik, A. Chanturiya, J. Green, J. Zimmerberg, The Hemifusion Intermediate and its Conversion to Complete Fusion: Regulation by Membrane Composition, 1995.

[32] A.R. Viguera, M. Mencia, F.M. Goni, Time-resolved and equilibrium measurements of the effects of poly(ethylene glycol) on small unilamellar phospholipid vesicles, Biochemistry. 32 (1993). https://doi.org/10.1021/bi00065a024.

[33] N.T. Ktistakis, S.A. Tooze, Digesting the Expanding Mechanisms of Autophagy, Trends in Cell Biology. 26 (2016) 624–635. https://doi.org/10.1016/j.tcb.2016.03.006.

[34] Z. Antón, A. Landajuela, J.H. Hervás, L.R. Montes, S. Hernández-Tiedra, G. Velasco, F.M. Goñi, A. Alonso, Human Atg8-cardiolipin interactions in mitophagy: Specific properties of LC3B, GABARAPL2 and GABARAP, Autophagy. 12 (2016) 2386–2403. https://doi.org/10.1080/15548627.2016.1240856.

[35] M.B. Ruiz-Argüello, G. Basáñez, F.M. Goñi, A. Alonso, Different Effects of Enzyme-generated Ceramides and Diacylglycerols in Phospholipid Membrane Fusion and Leakage, Journal of Biological Chemistry. 271 (1996) 26616–26621. https://doi.org/10.1074/jbc.271.43.26616.

[36] A.-V. Villar, A. Alonso, F.M. Goñi, Leaky Vesicle Fusion Induced by Phosphatidylinositol-Specific Phospholipase C: Observation of Mixing of Vesicular Inner Monolayers, Biochemistry. 39 (2000). https://doi.org/10.1021/bi992515c.

[37] J.L. Nieva, F.M. Goni, A. Alonso, Liposome fusion catalytically induced by phospholipase C, Biochemistry. 28 (1989). https://doi.org/10.1021/bi00444a032.

[38] T. Nishimura, S.A. Tooze, Emerging roles of ATG proteins and membrane lipids in autophagosome formation, Cell Discovery. 6 (2020). https://doi.org/10.1038/s41421-020-0161-3.

[39] T.J. Melia, A.H. Lystad, A. Simonsen, Autophagosome biogenesis: From membrane growth to closure, Journal of Cell Biology. 219 (2020). https://doi.org/10.1083/JCB.202002085.

[40] S. Martens, D. Fracchiolla, Activation and targeting of ATG8 protein lipidation, Cell Discovery. 6 (2020). https://doi.org/10.1038/s41421-020-0155-1.

[41] Y. Ichimura, Y. Imamura, K. Emoto, M. Umeda, T. Noda, Y. Ohsumi, In vivo and in vitro reconstitution of Atg8 conjugation essential for autophagy, Journal of Biological Chemistry. 279 (2004) 40584–40592. https://doi.org/10.1074/jbc.M405860200.

[42] T. Maruyama, J.M. Alam, T. Fukuda, S. Kageyama, H. Kirisako, Y. Ishii, I. Shimada, Y. Ohsumi, M. Komatsu, T. Kanki, H. Nakatogawa, N.N. Noda, Membrane perturbation by lipidated Atg8 underlies autophagosome biogenesis, Nature Structural and Molecular Biology. 28 (2021) 583–593. https://doi.org/10.1038/s41594-021-00614-5.

Table 1. Initial rates of the various LC3C-promoted effects, as recorded with the various biophysical techniques.

Units are s^{-1}. Figures are mean values ± S.E., n = 3. Note that the data were obtained using very different techniques, thus they are not always directly comparable. Data in the left-hand column can always be compared with the corresponding figures in the right-hand column. Within each column, only data obtained using the same technique can be compared.

	Monolayer (PE)	**Monolayer (PEmal)**
Insertion in monolayer (LC3C G126C)	0.42 ± 0.10	1.03 ± 0.23
Insertion in monolayer (LC3C)	0.20 ± 0.02	0.26 ± 0.04
	SUV (PEmal)	**LUV (PEmal)**
Vesicle aggregation (LC3C G126C)	0.117 ± 0.040	0.022 ± 0.007
Total lipid mixing (LC3C G126C)	21.8 ± 2.18	4.70 ± 0.91
Inner lipid mixing (LC3C G126G)	9.44 ± 1.52	2.83 ± 0.89
Total lipid mixing (LC3C)	2.97 ± 0.92	0.08 ± 0.02
Inner lipid mixing (LC3C)	0.93 ± 0.79	0.25 ± 0.27
Contents release (LC3C G126C)	26.5 ± 5.11	33.9 ± 11.1
Contents release (LC3C)	1.65 ± 0.22	0.85 ± 0.12

FIGURE LEGENDS

Fig. 1. LC3C surface-active properties and interaction with lipid monolayers in the Langmuir balance. (A,B) Time courses of surface pressure change at the air-buffer interface upon injection (at time 2 min) of LC3C or LC3C G126C at various concentrations into the buffer (NaCl 150 mM, 50 mM TRIS, pH 7.5). (C) The change in surface pressure $\Delta\pi$ under equilibrium conditions, as a function of protein concentration, average values, n = 3. (D-G) Changes in surface pressure of lipid monolayers, initially at $\pi \approx 20$ mN/m, upon injection of 2 µM LC3C (D,E) or LC3C G126C (F,G) into the subphase. Monolayers containing PC:DOPE:PI (35:55:10) (D,F) or PC:DOPE:PEmal:PI (35:25:30:10) (E,G).

Fig. 2. LC3C G126C interacts with PEmal. Vesicle flotation assay performed with small (SUV) or large unilamellar vesicles (LUV). LC3C or LC3C G126C (10 µM) were incubated with liposomes (3 mM) containing PC:DOPE:PEmal:PI (35:25:30:10) for 1 h, then centrifuged in a sucrose gradient. (A) SDS-PAGE gel stained with Coomassie Blue showing the four fractions derived from the sucrose gradient, bottom to top from left to right. The protein fraction recovered from the two top fractions was considered as vesicle bound. (B) Percent fractions of vesicle-bound protein in experiments as shown in (A). Empty bars: LUV. Filled bars: SUV. Average values of 3 measurements ± S.D.

Fig. 3. Chemical conjugation of LC3C G126C to PEmal. The lipidated and non-lipidated protein fractions could be separated by SDS-PAGE. (A) Small (SUV) or (B) large unilamellar vesicles (LUV) (0.4 mM) containing different proportions of PEmal (0 %, 20 %, 30 %) were incubated with LC3C G126C (5 µM). Aliquots were retrieved at different time points and the percentage of PEmal-bound protein was quantitated using SDS-PAGE gels stained with Coomassie Blue. Average values of 3 measurements ± S.D.

Fig. 4. Membrane aggregation induced by LC3C G126C. Vesicle membrane aggregation was followed through changes in vesicle suspension turbidity (absorbance at 400 nm). (A) SUV, or (B) LUV composed of PC:DOPE:PEmal:PI (35:25:30:10) (0.4 mM) were incubated at 37ºC for 5 min, then LC3C or LC3C G126C (5µM) was added. The arrow indicates protein addition.

Fig. 5. LC3C G126C-induced vesicle aggregation analyzed by cryo-EM. (A,B) LUV composed of PC:DOPE:PEmal:PI (35:25:30:10 mol ratio) (0.4 mM) and incubated at 37ºC with LC3C G126C (5µM). (C) Similar LUV incubated with LC3C. (D) Control vesicles, imaged in the absence of protein. Bar: 100 nm. The same scale was used in all images. Representative images of each condition, additional images can be found in the gallery (Supplementary Fig. S4).

Fig. 6. Lipid mixing induced by LC3C G126C. Liposomes composed of PC:DOPE:PEmal:PI (35:25:30:10 mol ratio) and of PC:DOPE:PEmal:PI:PE-NBD:PE-Rho (35:25:30:10:1.5:1.5 mol ratio) were mixed in a 9:1 ratio (0.4 mM total lipid concentration). The mixture was incubated for 5 min at 37 ºC, then the protein (LC3C or LC3C G126C) (5 µM) was added (arrow). Total and inner-monolayer lipid mixing were separately recorded, as detailed under Methods.

Fig. 7. Release of vesicle contents induced by LC3C or LC3C G126C. The ANTS/DPX assay was used to assess vesicle contents leakage. Liposomes containg PC:DOPE:PEmal:PI (35:25:30:10) (0.4 mM) were incubated for 5 min at 37 ºC, then 5 µM protein (LC3C or LC3C G126C) was added (arrow).

SUPPLEMENTARY FIGURE LEGENDS

Figure S1. The secondary structures of LC3C and LC3C G126C are virtually identical. A) The secondary structures of LC3C and LC3C G126C were examined using circular dichroism in System Buffer (50 mM Tris, 150 mM, pH 7.5). Each line corresponds to an accumulation of 40 scans. B) Protein stability was measured by circular dichroism along a 20-90 ºC temperature range in a low-salt buffer (5 mM Tris, 15 mM NaCl, pH 7.5). Melting points are 58ºC and 58.6 ºC respectively.

Fig. S2. Absence of LC3C or LC3C G126C interaction with vesicles not containing PEmal. LC3C or LC3C G126C (10µM) were incubated with liposomes containing PC:DOPE:PI (35:55:10) (3 mM) for 1 h, then centrifuged in a sucrose gradient. The SDS-PAGE gels stained with Coomassie Blue show the four fractions derived from the sucrose gradient, bottom to top from left to right. The protein fraction recovered from the two bottom fractions was considered as non vesicle-bound.

Fig. S3. Membrane aggregation assays. Vesicle membrane aggregation was followed through changes in vesicle suspension turbidity (absorbance at 400 nm). (A) SUV, or (B) LUV composed of PC:DOPE:PI (35:55:10) (0.4 mM) were incubated at 37 ºC for 5 min, then LC3C or LC3C G126C (5µM) was added (arrow). No aggregation activity was observed under conditions not allowing protein binding to PE.

Fig. S4. LC3C G126C-induced vesicle aggregation analyzed by cryo-EM: a gallery of images. (A1-A6) LUV composed of PC:DOPE:PEmal:PI (35:25:30:10 mol ratio) and incubated at 37ºC with LC3C G126C. (B1-B6) Similar LUV incubated with LC3C. (C1-C6) Control vesicles, imaged in the absence of protein. Bar: 100 nm. The same scale was used in all images. For A and B the protein/lipid mol ratio was 1/40.

Fig. S5. Absence of observable lipid mixing induced by LC3C or LC3 G126C when PEmal is not present in the bilayers. Liposomes of PC:DOPE:PI (35:55:10) and PC:DOPE:PI:PE-NBD:PE-Rho (35:55:10:1,5:1,5) were mixed at 9:1 proportion (0.4 mM total lipid concentration). The mixture was incubated for 5 min at 37 ºC, then 5 µM protein (LC3C or LC3C G126C) was added (arrow).

Fig. S6. Release of vesicle contents induced by LC3C or LC3C G126C. The ANTS/DPX assay was used to assess vesicle contents leakage. Liposomes containing PC:DOPE:PI (35:55:10) (0.4 mM) were incubated for 5 min at 37 ºC, then 5 µM protein (LC3C or LC3C G126C) was added (arrow).

FIGURES

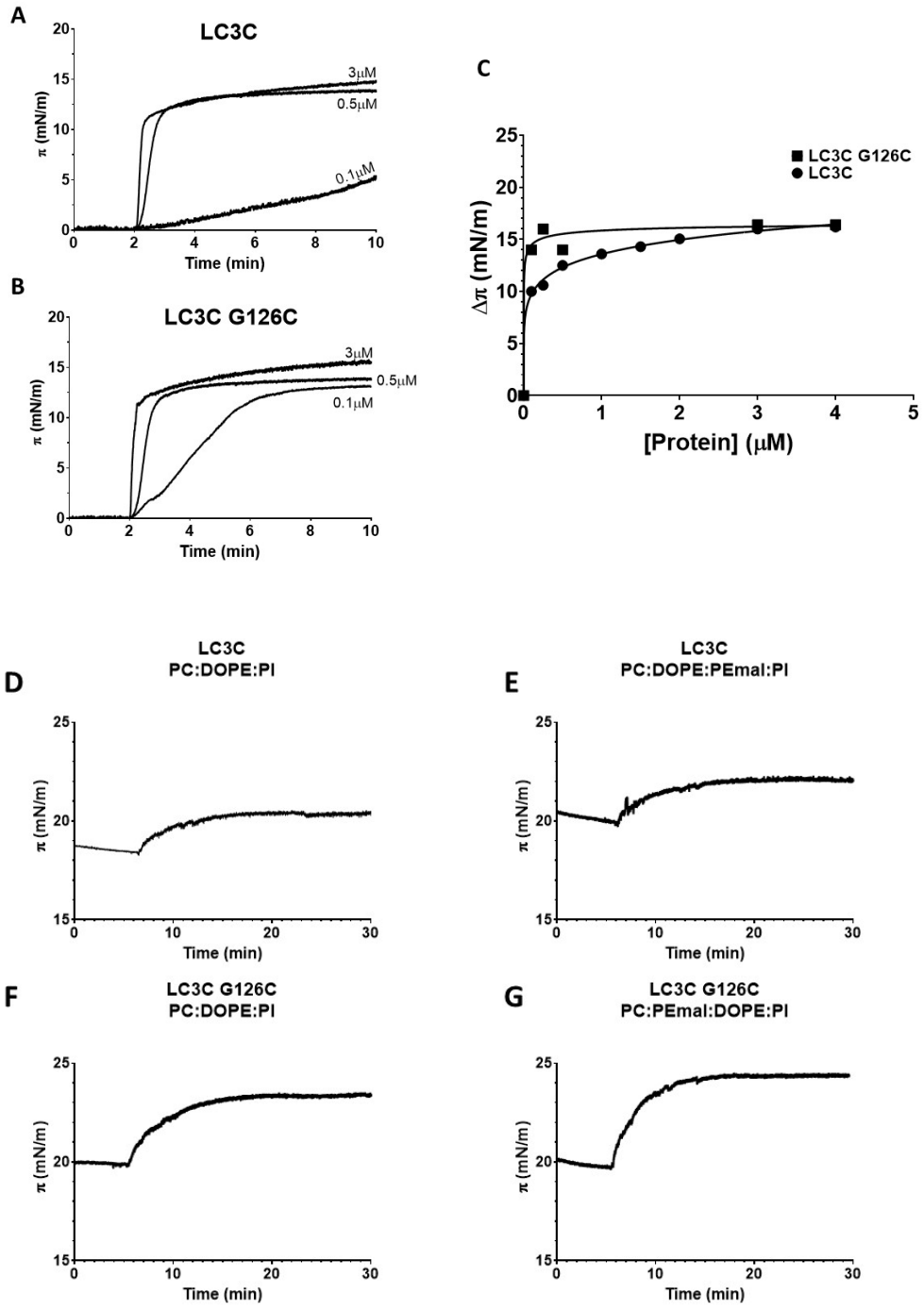

Figure 1. LC3C surface-active properties and interaction with lipid monolayers in the Langmuir balance. (A,B) Time course of surface pressure change at the air-buffer interface upon injection (at time 2 min) of LC3C or LC3C G126C at various concentrations into the buffer (NaCl 150 mM, 50 mM TRIS). (C) The change in surface pressure Δπ under equilibrium conditions, as a function of protein concentration. (D-G) Changes in surface pressure of lipid monolayers, initially at π ≈ 20 mN/m, upon injection of 2 μM of LC3C (D,E) or LC3C G126C (F,G) into the subphase. Monolayers containing PC:DOPE:PI (35:55:10) (D,F) or PC:DOPE:PEmal:PI (35:25:30:10) (E,G). Representative curves of n=3.

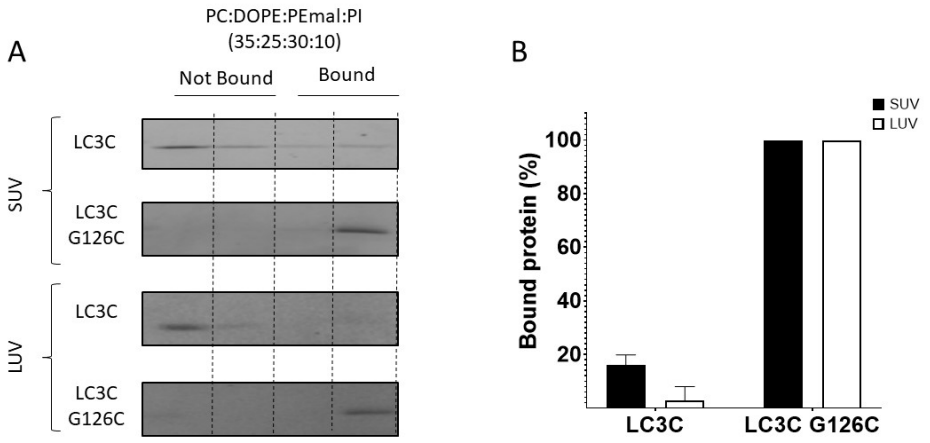

Figure 2. LC3C G126C interacts with PEmal. Vesicle flotation assay performed with small (SUV) and large unilamellar vesicles (LUV). LC3C or LC3C G126C (10 µM) were incubated with liposomes (3 mM) containing PC:DOPE:PEmal:PI (35:25:30:10) for 1 h, then centrifuged in a sucrose gradient. (A) SDS-PAGE gel stained with Coomassie Blue corresponding to the four fractions derived from the sucrose gradient, bottom to top from left to right. The protein fraction recovered from the two top fractions was considered as vesicle bound. (B) Percent fractions of vesicle-bound protein in experiments as shown in (A). Empty bars: LUV. Filled bars: SUV. Average values of 3 measurements ± S.D.

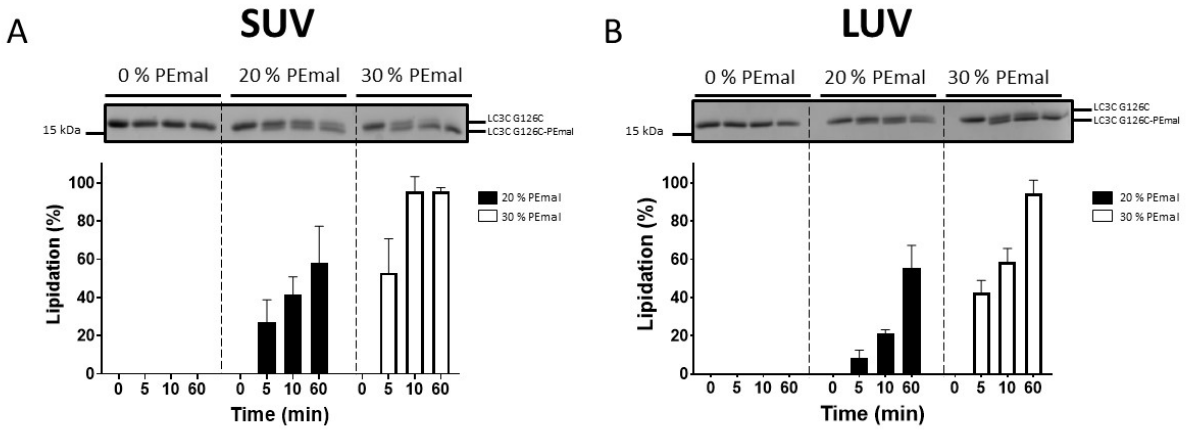

Figure 3. Chemical conjugation of LC3C G126C to PEmal. The lipidated and non-lipidated protein fractions could be separated by SDS-PAGE. (A) Small (SUV) or (B) large unilamellar vesciles (LUV) (0.4 mM) containing different proportions of PEmal (0 %, 20 %, 30 %) were incubated with LC3C G126C (5 µM). Aliquots were retrieved at different time points and the percentage of PEmal-bound protein was quantitated using SDS-PAGE gels stained with Coomassie Blue. Full bars: 20% PEmal. Empty bars: 30% PEmal. Average values of 3 measurements ± S.D.

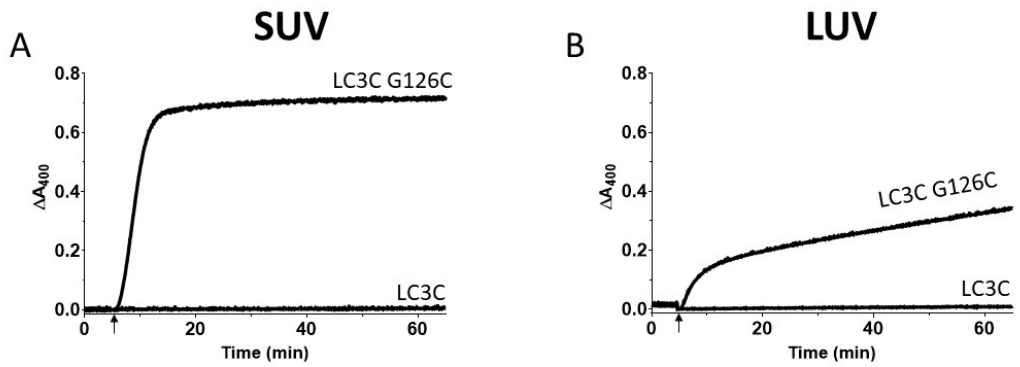

Figure 4. Membrane aggregation induced by LC3C G126C. Vesicle membrane aggregation was followed through changes in vesicle suspension turbidity (absorbance at 400 nm). (A) SUV, or (B) LUV composed of PC:DOPE:PEmal:PI (35:25:30:10) (0.4 mM) were incubated at 37ºC for 5 min, then LC3C or LC3C G126C (5µM) was added. The arrow indicates when the protein is added. Representative results of 3 independent mesurements.

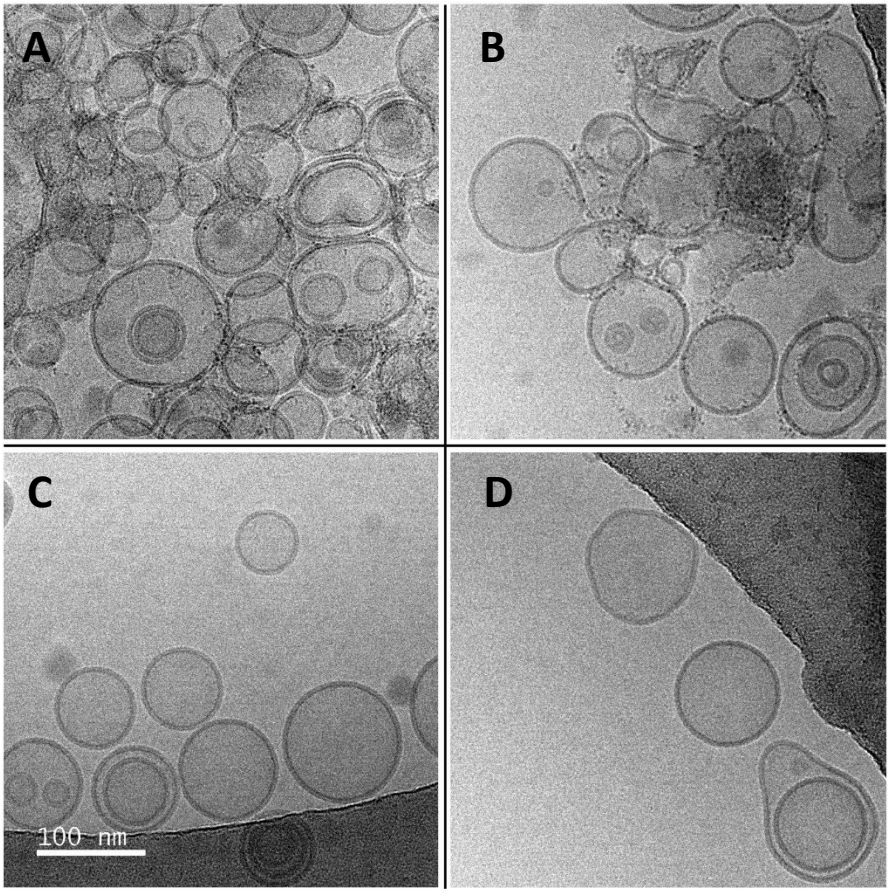

Figure 5. LC3C G126C-induced vesicle aggregation analyzed by cryo-EM. (A,B) LUV composed of PC:DOPE:PEmal:PI (35:25:30:10 mol ratio) (0.4 mM) and incubated at 37ºC with LC3C G126C (5µM). (C) Similar LUV incubated with LC3C. (D) Control vesicles, imaged in the absence of protein. Bar: 100 nm. The same scale was used in all images. Representative images of each conditions, more image can be found in the gallery (Fig. S4).

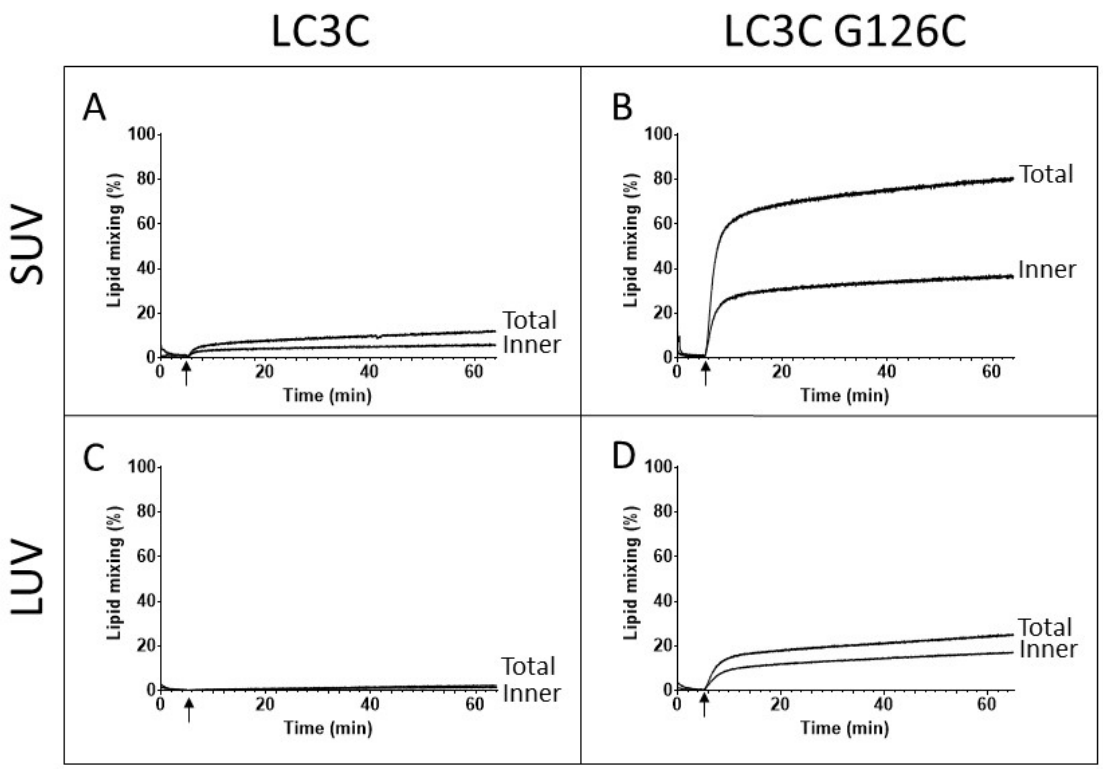

Figure 6. Lipid mixing induced by LC3C G126C. Liposomes composed of PC:DOPE:PEmal:PI (35:25:30:10 mol ratio) and of PC:DOPE:PEmal:PI:PE-NBD:PE-Rho (35:25:30:10:1.5:1.5 mol ratio) were mixed in a 9:1 ratio (0.4 mM). The mixture was incubated for 5 minutes at 37ºC, then the protein (LC3C or LC3C G126C) (5 µM) was added. Total and inner-monolayer lipid mixing were separately recorded, as detailed under Methods. Representative curve of 3 independent measurements.

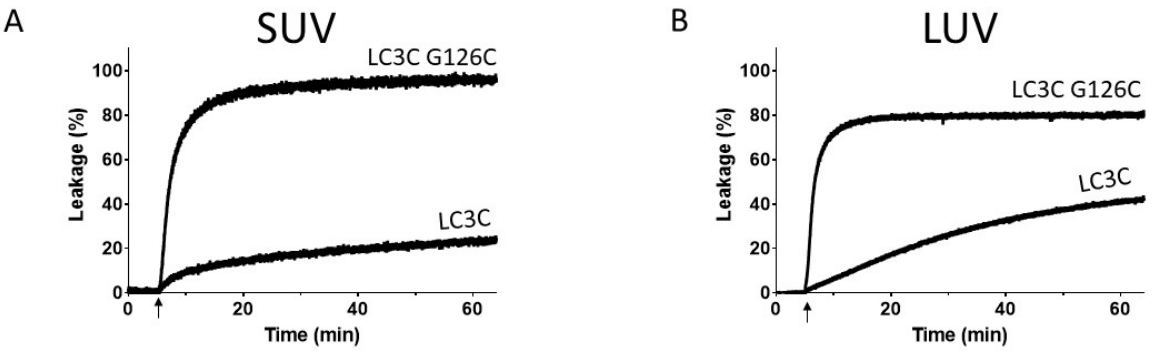

Figure 7. Release of vesicle contents induced by LC3C or LC3C G126C. The ANTS/DPX assay was used to assess vesicle contents leakage. Liposomes containg PC:DOPE:PEmal:PI (35:25:30:10) (0.4 mM) were incubated for 5 min at 37ºC, then 5 µM protein (LC3C or LC3C G126C) was added. Representative results of 3 independent measurements.

Supplementary Figures

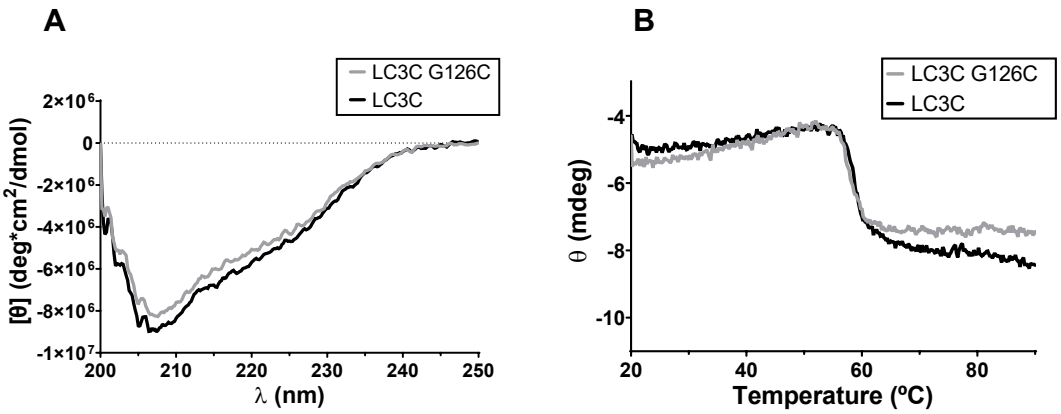

Figure S1. The secondary structures of LC3C and LC3C G126C are virtually identical. A) The secondary structures of LC3C and LC3C G126C were examined using circular dichroism in System Buffer (50 mM Tris, 150 mM, pH 7.5). Each line corresponds to an accumulation of 40 scans. B) Protein stability was measured by circular dichroism along a 20-90 ºC temperature range in a low-salt buffer (5 mM Tris, 15 mM NaCl, pH 7.5). Melting point are 58 ºC and 58.6 ºC respectively.

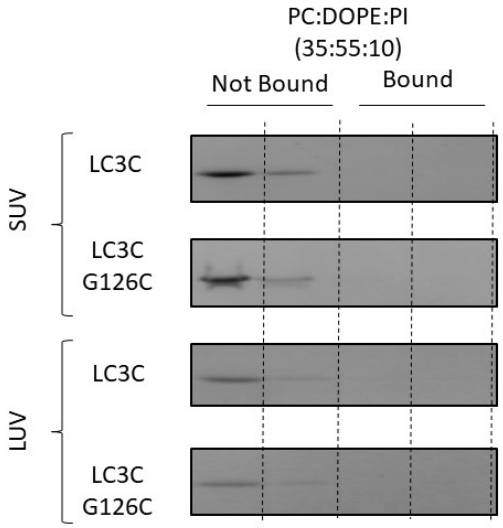

Figure S2. Lack of LC3C or LC3C G126C interaction with vesicles not containing PEmal. LC3C or LC3C G126C (10µM) were incubated with liposomes containing PC:DOPE:PI (35:55:10) (3 mM) for 1 h, then centrifuged in a sucrose gradient. The SDS-PAGE gels stained with Coomassie Blue corresponds to the four fractions derived from the sucrose gradient, bottom to top from left to right. The protein fraction recovered from the two bottom fractions was considered as non vesicle-bound. Representative SDS-PAGE gels of 3 independent repetitions.

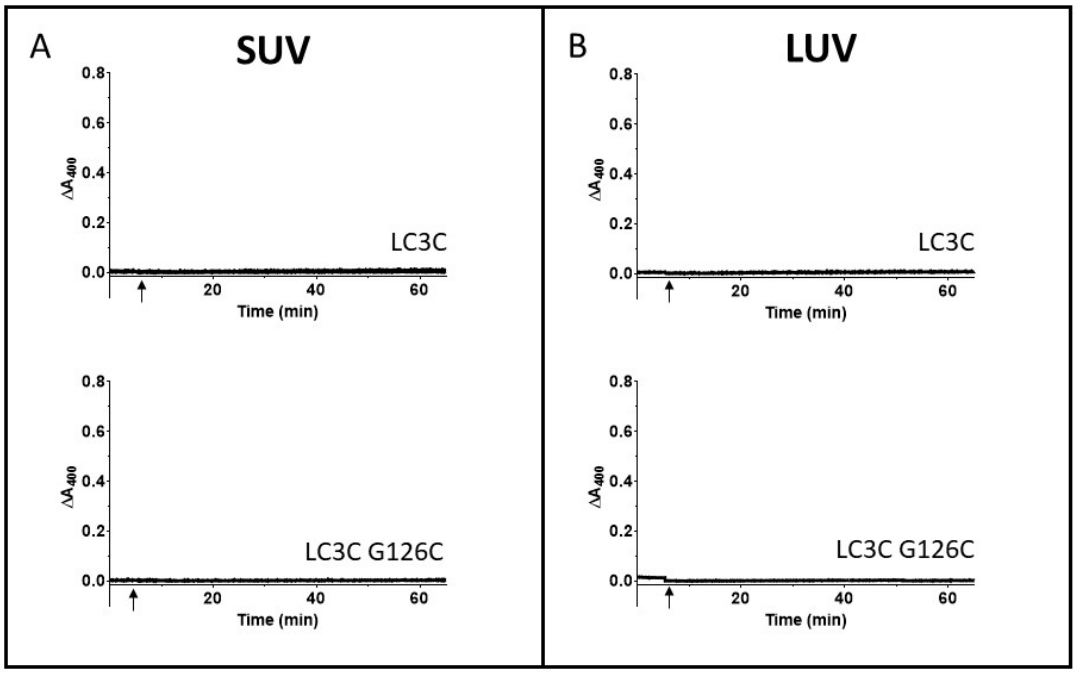

Figure S3. Membrane aggregation assays. Vesicle membrane aggregation was followed through changes in vesicle suspension turbidity (absorbance at 400 nm). (A) SUV, or (B) LUV composed of PC:DOPE:PI (35:55:10) (0.4 mM) were incubated at 37 ºC for 5 min, then LC3C or LC3C G126C (5µM) was added. No aggregation activity was observed under conditions not allowing protein binding to PE.

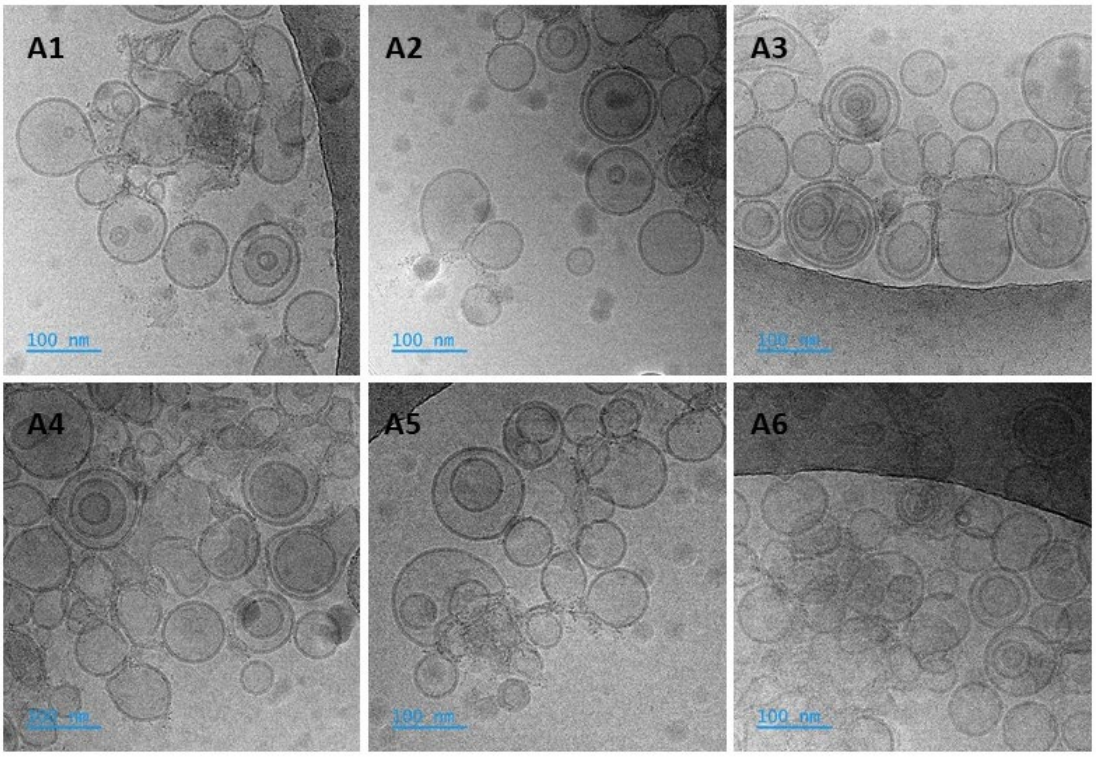
A1
100 nm
A2
100 nm
A3
100 nm
A4
100 nm
A5
100 nm
A6
100 nm

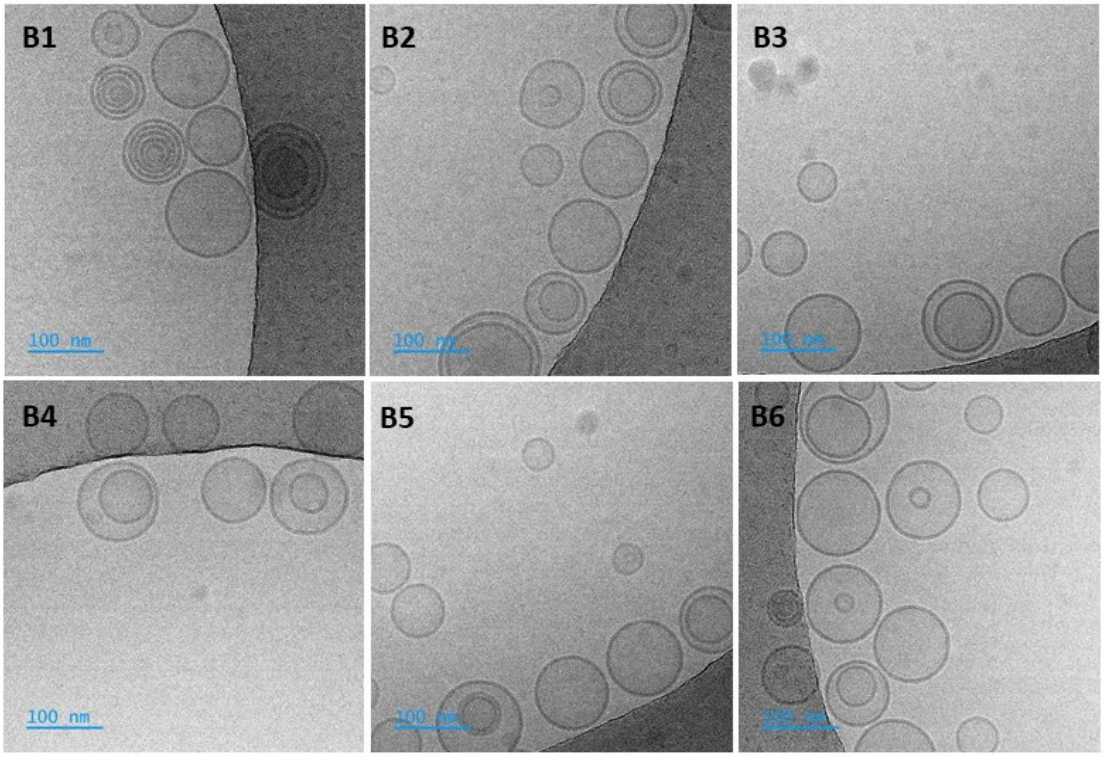
B1
100 nm
B2
100 nm
B3
100 nm
B4
100 nm
B5
100 nm
B6
100 nm

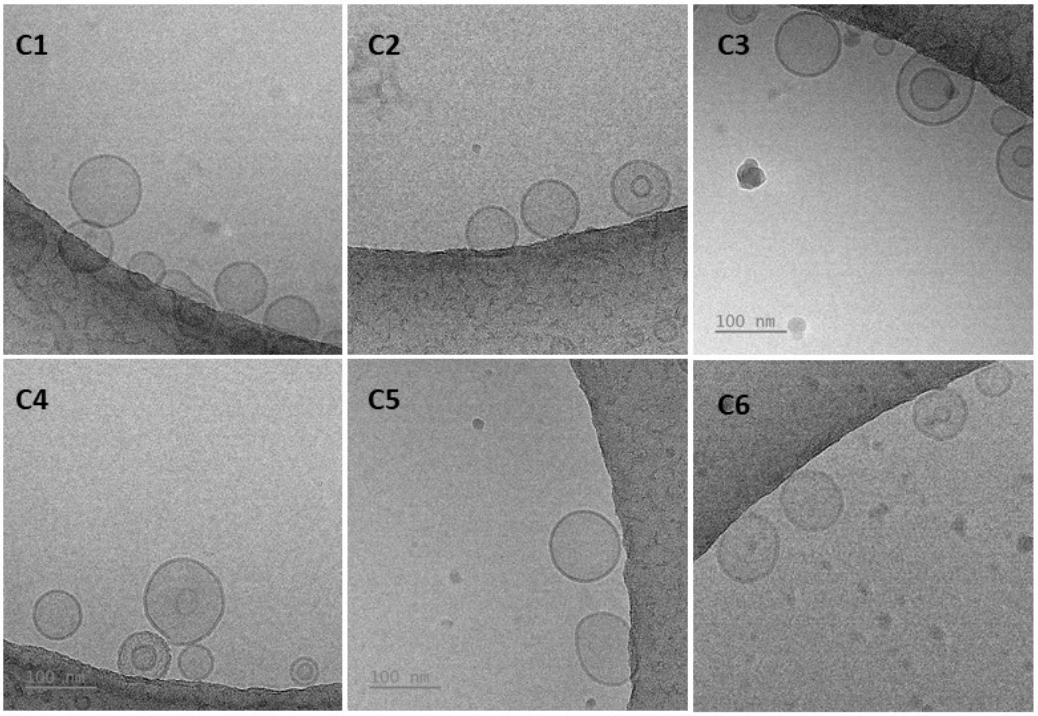

Figure S4. LC3C G126C-induced vesicle aggregation analyzed by cryo-EM: a gallery of images. (A1-A6) LUV composed of PC:DOPE:PEmal:PI (35:25:30:10 mol ratio) and incubated at 37ºC with LC3C G126C. (B1-B6) Similar LUV incubated with LC3C. (C1-C6) Control vesicles, imaged in the absence of protein. Bar: 100 nm. The same scale was used in all images. For A and B, the protein/lipid ratio was 1/40.

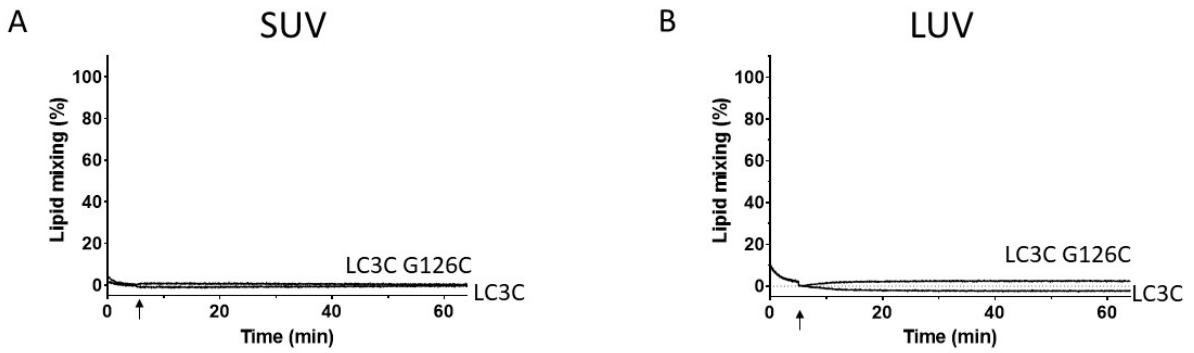

Figure S5. Absence of observable lipid mixing induced by LC3C or LC3C G126C when PEmal is not present in the bilayers. Liposomes of PC:DOPE:PI (35:55:10) and PC:DOPE:PI:PE-NBD:PE-Rho (35:55:10:1.5:1.5) were mixed at a 9:1 proportion (0.4 mM). The mixture was incubated for 5 minutes at 37 ºC, then 5 µM protein (LC3C or LC3C G126C) was added.

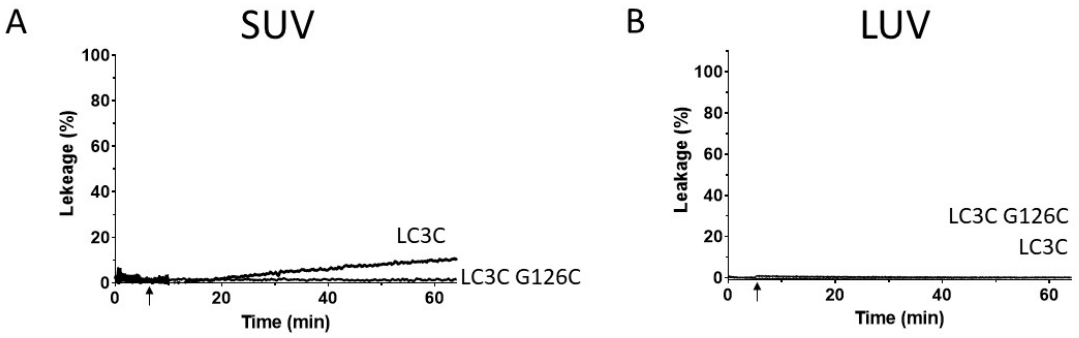

Figure S6. Release of vesicle contents induced by LC3C or LC3C G126C. The ANTS/DPX assay was used to assess vesicle contents leakage. Liposomes containing PC:DOPE:PI (35:55:10) (0.4 mM) were incubated for five minutes at 37 ºC, then 5 µM protein (LC3C or LC3C G126C) was added.